J. Fluid Mech. (1981), *vol.* 108, *pp.* 485–499
Printed in Great Britain

Enhanced sedimentation in narrow tilted channels

By ERIC HERBOLZHEIMER† AND ANDREAS ACRIVOS
Department of Chemical Engineering, Stanford University, Stanford, CA 94305

(Received 6 May 1980 and in revised form 29 October 1980)

The analysis of Acrivos & Herbolzheimer (1979) is extended to describe the sedimentation of dilute suspensions in tilted two-dimensional channels in which the spacing between the plates is small compared with their length. The theory assumes that the flow is laminar and that the suspension consists of monodisperse spherical beads having small particle Reynolds number. Expressions for the flow fields in the clear-fluid region and in the suspension, as well as for the location of the interface separating these two regions, are obtained asymptotically in the limit of $\Lambda \gg 1$ with $R\Lambda^{-\frac{1}{3}} \ll 1$, where R and Λ are as defined in the previous work. The present analysis differs from that given earlier in that the aspect ratio, i.e. the ratio of the height of the suspension to the channel width, is now taken to be $O(\Lambda^{\frac{1}{3}})$ rather than $O(1)$ as was the case before. Under these conditions, the solution of the time-dependent equations leads to the surprising prediction that the clear-fluid layer which forms beneath the downward-facing plate attains a steady shape only along the lower portion of the channel while, in contrast, its thickness increases with time for locations along the channel that are above some critical point. Because of this transient behaviour, the well-known Ponder–Nakamura–Kuroda (PNK) formula overestimates the rate at which the top of the suspension region falls with time; however, the PNK results for the volumetric settling rate still hold under the conditions considered in this paper. It is shown that this discontinuity in the interface shape can be suppressed in continuous settling systems but only if the feed and withdrawal locations are chosen properly.

Batch sedimentation experiments were conducted in a channel with parallel flat walls under the following sets of conditions: $H_0/b \approx 90$, $5^\circ \leqslant \theta \leqslant 45^\circ$, $0{\cdot}01 \leqslant c_0 \leqslant 0{\cdot}025$, $1{\cdot}7 \times 10^7 < \Lambda < 3{\cdot}5 \times 10^7$, and $1{\cdot}8 < R < 2{\cdot}1$, where θ is the angle of inclination of the vessel from the vertical, and c_0 is the initial volume fraction of solids in the suspension. The experimental observations were found to be in excellent agreement with the theoretical predictions.

1. Introduction

Boycott (1920) was the first to report that, if a suspension is left to stand in a narrow tube, the particles sediment much faster if the tube is inclined than when it is vertical. A detailed description of the 'Boycott effect' as well as a summary of the earlier papers on the subject were presented in a recent communication (Acrivos & Herbolzheimer 1979, henceforth referred to as I).

In addition to being of interest in its own right, the 'Boycott effect' has obvious

† Present address: Chemical Engineering, California Institute of Technology, Pasadena, CA 91125.

practical potential for greatly increasing the efficiency of gravity-settling operations used in industry. Before this potential can be realized, however, it is important that a quantitative theory be developed for describing the convective phenomena that arise during this process. Such a theory was presented in I for the case of two-dimensional flows in vessels having $O(1)$ aspect ratios. This theory is extended in the present paper to the case of settling in tilted channels for which the aspect ratio, i.e. the ratio of the height of the suspension to the spacing between the plates, is very large. Such vessels are of greater interest from a practical standpoint because they correspond to the largest enhancement of the settling rate.

As in I, the suspensions considered are composed of identical spheres which are small enough so that the particle Reynolds number – based on the velocity of the particles relative to that of the surrounding fluid – is much less than unity. Under these conditions, the expression for the instantaneous volumetric rate at which particle-free fluid is formed is given by equation (2.10) of I which verifies the corresponding prediction obtained by Ponder (1925) and independently by Nakamura & Kuroda (1937) (henceforth denoted by PNK) using an *ad hoc* argument. This result is independent of the details of the flow. It was further shown in I that, aside from the geometry of the vessel, a complete description of the settling process is governed by two dimensionless parameters: R, a sedimentation Reynolds number, and Λ, the ratio of a sedimentation Grashof number to R,

$$\left.\begin{aligned} R &\equiv \frac{lv_0\rho_f}{\mu} = \tfrac{2}{9}la^2\rho_f\frac{(\rho_s-\rho_f)}{\mu^2}gf(c_0), \\ \Lambda &\equiv \frac{l^2g(\rho_s-\rho_f)c_0}{\mu v_0} = \frac{9}{2}\left(\frac{l}{a}\right)^2\frac{c_0}{f(c_0)}, \end{aligned}\right\} \tag{1.1}$$

where l is a characteristic length of the macroscale motion and $v_0 = u_0 f(c_0)$ is the average vertical settling velocity of a sphere in the suspension if c, the volume fraction of solids, equals its initial value, c_0. The Stokes settling velocity of the spheres is given by

$$u_0 = \tfrac{2}{9}a^2\frac{\rho_s-\rho_f}{\mu}g, \tag{1.2}$$

and $f(c)$ is a monotonically decreasing function which accounts for interactions between particles, being unity for $c = 0$. The pure fluid viscosity is μ, its density is ρ_f, ρ_s is the density of the spheres, a is their radius, and g is the gravitational constant. Since, in most cases of interest, Λ is $O(10^6)$–$O(10^8)$, while R is only $O(1)$–$O(10^2)$, an asymptotic analysis for determining the details of the motion was developed in I by taking $\Lambda \gg 1$ with $R\Lambda^{-\frac{1}{3}} \leqslant O(1)$. It was shown that the region of pure fluid beneath the downward-facing surface of the vessel forms a thin rapidly flowing layer whose thickness scales as $\Lambda^{-\frac{1}{3}}$ and in which the longitudinal velocity scales as $\Lambda^{\frac{1}{3}}$. For $H/b \ll \Lambda^{\frac{1}{3}}$, with H and b being, respectively, the height of the suspension and the spacing between the plates of the channel, this clear-fluid layer is much thinner than b and attains a steady shape in a time interval that is small compared with the characteristic time for settling of the suspension. Hence, all of the pure fluid which is formed accumulates above the essentially horizontal interface at the top of the suspension region, and, as shown in I, the PNK theory correctly predicts the rate of downward

descent of this interface, with an error of $O(\Lambda^{-\frac{1}{3}})$. For the common geometry of parallel flat plates, we therefore obtain that

$$\frac{dH}{dt} = -v_0\left(1+\frac{H}{b}\sin\theta\right)+O(\Lambda^{-\frac{1}{3}}), \tag{1.3}$$

where θ is the angle of inclination of the channel from the vertical.

In contrast, when $H/b \sim O(\Lambda^{\frac{1}{3}})$ the clear-fluid layer beneath the downward-facing surface occupies an appreciable portion of the channel, and the analysis of I no longer holds. Surprisingly enough, this important case has not received any attention in the past even though (1.3) would suggest that a very large enhancement in the settling rate could be achieved under these conditions. For example, a very high capacity settling device could be produced by placing many closely spaced parallel plates within a larger tank so that the aspect ratio of each cell would be very large.

In the present paper we shall extend our earlier work and shall develop an asymptotic solution to the flow equations under the same set of conditions as in I except that H/b will be taken as $O(\Lambda^{\frac{1}{3}})$. In order to clarify the presentation, we shall restrict our attention to the sedimentation of dilute suspensions in two-dimensional channels having parallel flat walls. The extension of our analysis to more general geometries and to non-dilute suspensions is straightforward (Herbolzheimer 1980). In the next section we shall formulate the mathematical problem and shall obtain expressions for the velocity profile while, in § 3, the equation governing the time-dependent interface position will be solved analytically for the case of batch sedimentation. It will be shown that, surprisingly, the clear-fluid layer which forms beneath the downward-facing plate attains a steady shape only along the lower portion of the channel while, in contrast, its thickness increases with time for locations along the channel that are above some critical point. In other words, when viewed as a function of distance along the channel, the thickness of the clear-fluid layer becomes discontinuous. Under these conditions the PNK theory accurately predicts the volumetric settling rate, but the corresponding result for the motion of the top of the suspension, i.e. (1.3), no longer holds. It is shown in § 4, however, that the discontinuous behaviour of the clear-fluid layer can be suppressed in continuous settling systems if the feed and withdrawal are chosen properly. Finally, it will be seen that the analytical predictions compare favourably with the results of batch settling experiments which were performed in our laboratory.

2. General formulation

As was discussed in § 2 of I, there are three regions to consider: (1) the particle-free layer; (2) the suspension region where $c \equiv c_0$ throughout the settling process;† and (3) the sediment layer along the upward-facing surface where c rises from c_0 to its maximum possible value. In contrast to the case of an $O(1)$ aspect ratio, the thickness of the sediment layer may become an appreciable fraction of the channel width when the spacing between the plates is small; nevertheless, its presence will be neglected in order to simplify the analysis. Although this approximation is accurate in the dilute

† The use of $c \equiv c_0$ within the suspension is justified if the latter is initially of uniform concentration and if the effect of particle interactions on the settling velocity of the spheres relative to the bulk average velocity depends only on the local concentration.

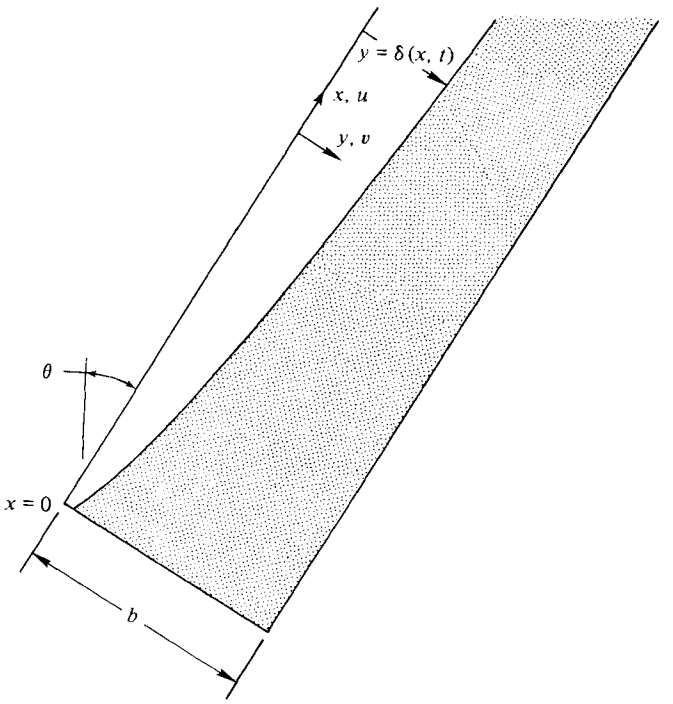

FIGURE 1. Expanded view showing the definition of the variables used in the analysis of the motion.

limit (cf. Herbolzheimer 1980), it could lead, in general, to quantitative differences between theory and experiments; however, the important qualitative features of the flow to be described below should apply to all situations.

We begin with the dimensionless averaged equations of motion and of continuity, i.e. equations (2.2) and (3.1) of I, which for both the pure fluid and suspension regions are

$$R\frac{D\mathbf{u}}{Dt} = -\nabla P - \Lambda\left(1-\frac{c}{c_0}\right)\mathbf{e} + \nabla^2\mathbf{u}, \tag{2.1}$$

and

$$\nabla.\mathbf{u} = 0, \tag{2.2}$$

where the $O(c_0)$ deviations of the suspension viscosity and of its density in the inertia terms from the corresponding pure-fluid values have been neglected in the dilute limit. In (2.1) and (2.2), $\mathbf{u}$ is the dimensionless average velocity of the suspension, ∇P is the dimensionless pressure gradient minus the hydrostatic pressure gradient due to suspension with volume fraction of solids c_0, and $\mathbf{e}$ is the unit vector in the direction of gravity. As in I, the equations have been rendered dimensionless using, respectively, H_0 (the initial height of the suspension), v_0, H_0/v_0 and $\mu v_0/H_0$ as the characteristic length, velocity, time, and pressure. Also, R and Λ are as defined in (1.1) except that H_0 replaces l. Finally, with these definitions, the dimensionless average particle velocity equals $\mathbf{u}+\mathbf{e}$.

We shall seek an asymptotic solution to these equations in the limit of $\Lambda \to \infty$ for settling between parallel plates. We define a co-ordinate system with x directed along the downward-facing plate of the channel and y perpendicular to it (see figure 1)

and with u and v the corresponding velocity components. With $b/H_0 \sim O(\Lambda^{-\frac{1}{3}})$, the length scale in the y direction is $O(\Lambda^{-\frac{1}{3}})$ in both the suspension and the pure fluid layers. Hence, on account of (2.1), the large bouyancy force in the pure-fluid layer must be balanced by the viscous forces, from which it follows that $u \sim O(\Lambda^{\frac{1}{3}})$. In turn, this implies from continuity that $v \sim O(1)$. Hence, we define the stretched variables

$$\tilde{y} = \Lambda^{\frac{1}{3}} y/\tilde{b}, \quad \tilde{u} = \Lambda^{-\frac{1}{3}} u, \quad \tilde{v} = v, \quad \tilde{P} = P/\Lambda, \tag{2.3}$$

where

$$\tilde{b} \equiv \Lambda^{\frac{1}{3}} b/H_0$$

is an $O(1)$ quantity by definition. Also, we let $\tilde{y} \equiv \tilde{\delta}(x,t)$ be the equation for the interface between the pure fluid and the suspension. In terms of the stretched variables, the momentum and continuity equations take then the familiar form of lubrication theory,

$$\frac{1}{\tilde{b}^2}\frac{\partial^2 \tilde{u}}{\partial \tilde{y}^2} - \frac{\partial \tilde{P}}{\partial x} + \left(1 - \frac{c}{c_0}\right)\cos\theta + O(R\Lambda^{-\frac{1}{3}}) = 0, \tag{2.4a}$$

$$\frac{\partial \tilde{P}}{\partial \tilde{y}} \sim O(\Lambda^{-\frac{1}{3}}) + O(R\Lambda^{-\frac{2}{3}}), \tag{2.4b}$$

and

$$\frac{\partial \tilde{u}}{\partial x} + \frac{1}{\tilde{b}}\frac{\partial \tilde{v}}{\partial \tilde{y}} = 0. \tag{2.4c}$$

These equations apply everywhere in the flow field except, of course, in small singular regions near the ends of the suspension where the characteristic length scale in the x direction is $O(\Lambda^{-\frac{1}{3}})$ so that derivatives in the x direction must also be retained. These regions have a small effect on the flow over most of the length of the channel, however, and can be neglected to leading order. For the sake of simplicity, let us restrict our attention to the case $R \sim O(1)$ so that the inertia terms, of order $R\Lambda^{-\frac{1}{3}}$, may also be neglected to leading order.

The y-momentum balance (2.4b) together with the normal stress balance at $\tilde{y} = \tilde{\delta}$ shows that $\tilde{P}$ is independent of $\tilde{y}$ to leading order. Hence, (2.4a) can be readily integrated to yield, after applying the boundary conditions of no-slip at the walls and continuity of velocity and shear stress at $\tilde{y} = \tilde{\delta}$,

$$\tilde{u} = \frac{6Q}{\tilde{b}}\tilde{y}(1-\tilde{y}) - \tilde{y}[(\tilde{\delta} + \tfrac{1}{2})\tilde{y} - \tilde{\delta}](1-\tilde{\delta})^2\tilde{b}^2\cos\theta, \tag{2.5a}$$

in the pure-fluid layer (i.e. for $0 \leqslant \tilde{y} \leqslant \tilde{\delta}$), and

$$\tilde{u} = \frac{6Q}{b}\tilde{y}(1-\tilde{y}) - (1-\tilde{y})[(\tfrac{3}{2} - \tilde{\delta})\tilde{y} - \tfrac{1}{2}]\tilde{\delta}^2\tilde{b}^2\cos\theta, \tag{2.5b}$$

in the suspension layer (i.e. for $\leqslant \tilde{y} \leqslant 1$). $Q(x,t)$ is the net flow rate of material across any plane of constant x and must satisfy the volume conservation condition

$$\frac{\partial Q(x,t)}{\partial x} = F(x,t) - V(x,t), \tag{2.6}$$

where $F(x,t)$ is the dimensionless flux at which new suspension is added into the channel at position x and $V(x,t)$ is the dimensionless flux at which pure fluid is removed through the upper wall. Of course, if the concentration distribution and stretchings employed in the present analysis are to remain valid, this new suspension must be

added directly to the suspension region with a velocity of $O(1)$. Under these conditions, the addition of the feed can be incorporated into the analysis either by modifying the continuity equation (2.4c), to include an $O(1)$ source term acting only in the suspension, or by changing the boundary conditions to allow for the flow of an $O(1)$ flux of suspension across the upward-facing wall. As will become apparent below, however, to leading order these modifications affect only the profile for $\tilde{v}$ in the suspension region, a quantity which is unimportant to the present degree of approximation. Hence, for the present purposes, the details of the feed at any value of x are unimportant and (2.5) applies for continuous as well as for batch systems. In general, concentrated sediment may also be removed at points along the channel but since this flux makes an $O(c_0)$ contribution to (2.6) it can be neglected to the present degree of approximation.

To complete the description of the flow field, it is necessary to determine the thickness of the clear-fluid layer, $\tilde{\delta}(x,t)$, by solving

$$\Lambda^{-\frac{1}{3}}\tilde{b}\frac{\partial\tilde{\delta}}{\partial t}+\tilde{b}\frac{\partial}{\partial x}\left\{\int_0^{\tilde{\delta}}\tilde{u}\,d\tilde{y}\right\}+V(x,t)=\sin\theta, \tag{2.7}$$

which results from applying the kinematic condition at the pure-fluid/suspension interface (cf. equation (3.4b) of I) and then integrating the continuity equation (2.4c) to evaluate $\tilde{v}$ at $\tilde{y}=\tilde{\delta}$. Finally, on account of (2.5a),

$$\tilde{b}\int_0^{\tilde{\delta}}\tilde{u}\,d\tilde{y}=(3-2\tilde{\delta})\,\tilde{\delta}^2Q(x,t)+\tfrac{1}{3}\tilde{\delta}^3(1-\tilde{\delta})^3\tilde{b}^3\cos\theta. \tag{2.8}$$

The use of pseudo-steady velocity profiles in deriving (2.7) is justified because the time derivatives in the momentum equation are $O(R\Lambda^{-\frac{2}{3}})$ and, therefore, play a negligible role relative to the other terms in (2.7).

When considered as mass balance over a thin slice of the clear-fluid layer (2.7) shows that, to leading order, a flux of fluid with magnitude $\sin\theta$ crosses the interface into the clear-fluid layer and that this flux must be balanced by the accumulation in the layer (i.e. $\Lambda^{-\frac{1}{3}}\tilde{b}\,\partial\tilde{\delta}/\partial t$), by the rate of change with respect to x of the net flow rate of fluid along the clear-fluid layer, or by a combination of these two effects. We shall investigate the solution of (2.7) for the two important cases of batch sedimentation and of steady-state continuous sedimentation.

3. Batch sedimentation

Since material is neither added to nor removed from the vessel during batch sedimentation, $F(x,t)$, $V(x,t)$ and $Q(x,t)$ all vanish and the equation governing the interface shape becomes

$$\frac{\partial\tilde{\delta}}{\partial\tau}+64\frac{\partial}{\partial\zeta}\{\tilde{\delta}^3(1-\tilde{\delta})^3\}=1, \tag{3.1}$$

where $\tau\equiv\Lambda^{\frac{1}{3}}t\sin\theta/\tilde{b}$ and $\zeta\equiv 192\,x\tan\theta/\tilde{b}^3$. To begin with, let us consider the possibility that, as was found in I for the case when the aspect ratio is $O(1)$, the interface along the clear-fluid layer attains a steady shape within a short initial time period, after which the only unsteadiness in the process is due to the vertical motion of the horizontal interface on top of the suspension. Integrating the steady form of (3.1) and solving for $\tilde{\delta}$, we obtain

$$\tilde{\delta}(\zeta)=\tfrac{1}{2}[1\pm(1-\zeta^{\frac{1}{3}})^{\frac{1}{2}}]. \tag{3.2}$$

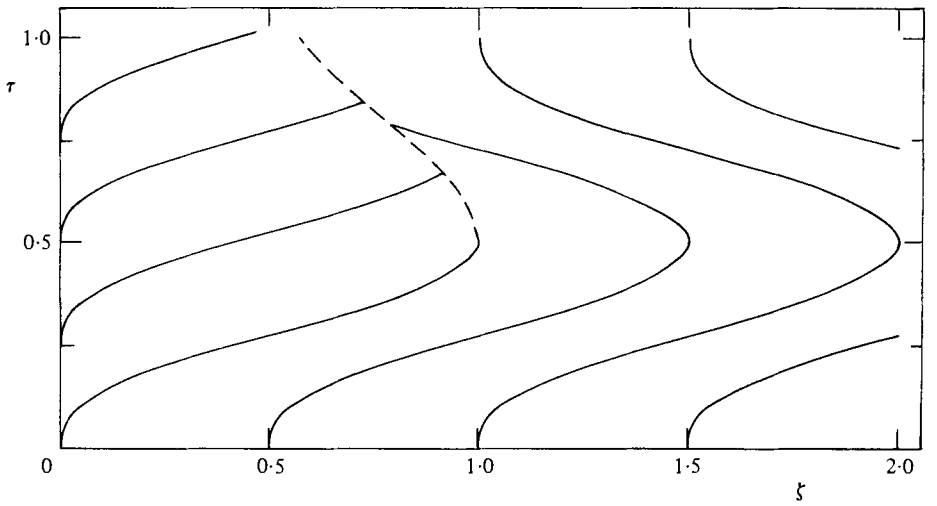

FIGURE 2. The characteristic map for determining the time-dependent behaviour of the thickness of the clear-fluid layer, $\delta(x, t)$, in vessels with large aspect ratios. The dashed line shows the position of the discontinuity in the layer thickness as a function of time.

Surprisingly, according to (3.2), real solutions for the steady interface shape exist only if $\zeta < 1$, i.e. for

$$x < x_c \equiv \frac{\tilde{b}^3}{192 \tan\theta}, \tag{3.3}$$

thereby implying that the interface may attain a steady shape only for $x < x_c$ while remaining transient for $x > x_c$. To determine whether such behaviour is possible we shall examine the solution of the time-dependent equation (3.1) using the method of characteristics.

Let us consider then the solution of (3.1) subject to the typical initial condition $\tilde{\delta}(\zeta, 0) = 0$, which corresponds to the vessel having been filled initially completely with suspension, and the boundary condition $\tilde{\delta}(0, \tau) = 0$ which is justified by matching the flow in the clear-fluid layer to that in the singular region at the end of the channel (cf. § 3 of I). For this case, we find that $\tilde{\delta} = \tau$ along all those characteristics crossing the ζ axis and that the shape of the characteristic with intercept $\zeta = \zeta_0$ is given by

$$\tilde{\delta} = \tau = \tfrac{1}{2}[1 - (1 - (\zeta - \zeta_0)^{\frac{1}{3}})^{\frac{1}{2}}] \quad \text{for} \quad \tau \leqslant \tfrac{1}{2} \tag{3.4a}$$

and

$$\tilde{\delta} = \tau = \tfrac{1}{2}[1 + (1 - (\zeta - \zeta_0)^{\frac{1}{3}})^{\frac{1}{2}}] \quad \text{for} \quad \tau \geqslant \tfrac{1}{2}. \tag{3.4b}$$

Similarly, for the characteristic crossing the τ axis at τ_0, we find

$$\tilde{\delta} = \tau - \tau_0 = \tfrac{1}{2}[1 - (1 - \zeta^{\frac{1}{3}})^{\frac{1}{2}}], \tag{3.5}$$

which is identical to the characteristic passing through the origin except for a shift in τ equal to the value of the τ intercept.

The time-dependent behaviour of the interface position can now be ascertained from the characteristic diagram shown in figure 2. At a given value of ζ, the thickness of the clear-fluid layer increases linearly with time until that characteristic is reached which crosses the origin; for later times, the interface is stationary for that ζ. Thus, for any $\tau < \frac{1}{2}$, the interface will be at its stationary position for all points below some

particular ζ while, above this point, it will be flat and be moving across the channel with a dimensionless velocity $\sin\theta$, the y component of the settling velocity of the particles. Unlike the case when the aspect ratio is $O(1)$, however, the characteristics which cross the ζ axis do not continue out to infinity but instead attain infinite slopes at $\tau = \frac{1}{2}$ and $\zeta = \zeta_0 + 1$; moreover, as τ increases beyond $\frac{1}{2}$, ζ decreases along these characteristics (cf. figure 2). Hence, for $\tau > \frac{1}{2}$, the characteristics which cross the τ axis will begin to intersect those which cross the ζ axis, and, since $\tilde{\delta} = \tau$ along the latter, while $\tilde{\delta} = \tau - \tau_0$ along the former, the thickness of the clear-fluid layer will be a discontinuous function of x.

The point of discontinuity first appears at $\zeta = 1$ and then propagates down the vessel with velocity $\Lambda^{\frac{1}{3}}\tilde{w}(\tau)$ in the negative x direction. This velocity is determined by noting that the differential mass balance (3.1) does not hold at the discontinuity, but must be replaced by a jump condition obtained from a mass balance in the clear-fluid layer about x_s, the position of the discontinuity. This balance requires that

$$\left[\tilde{b}\int_0^{\tilde{\delta}} (\tilde{u}+\tilde{w})\,d\tilde{y}\right]_{x_s} = 0,$$

which, since $\tilde{w}$ is independent of $\tilde{y}$, is equivalent to

$$-\tilde{w} = \Lambda^{-\frac{1}{3}}\frac{dx_s}{dt} = \frac{[\frac{1}{3}\tilde{b}^3\tilde{\delta}^3(1-\tilde{\delta})^3\cos\theta]_{x_s}}{[\tilde{\delta}]_{x_s}}, \tag{3.6}$$

where the square brackets denote the difference in the value of the enclosed quantity immediately above and below x_s. It is seen from the solution of (3.1) that immediately below x_s the interface is at its stationary position given by (3.5), evaluated at $\zeta = \zeta_s$, while, immediately above x_s, $\tilde{\delta}(\zeta_s, \tau) = \tau$. Substituting these results along with the definitions of ζ and τ into (3.6), we obtain

$$\frac{d\zeta_s}{d\tau} = \frac{[4\tau(1-\tau)]^3 - \zeta_s}{\tau - \frac{1}{2}[1-(1-\zeta_s^{\frac{1}{2}})^{\frac{1}{2}}]}, \tag{3.7}$$

with initial condition $$\zeta_s(\tfrac{1}{2}) = 1.$$

Equation (3.7) applies between $\tau = \frac{1}{2}$, when the discontinuity first appears, and $\tau = 1$, when the interface above x_s reaches the upward-facing surface. This initial-value problem was solved numerically and the solution is shown as the dashed line in figure 2. We note that $\zeta_s(1) = 0{\cdot}571$ which was confirmed in the experiments described in § 5. In actuality, a singular region with dimensions $O(\Lambda^{-\frac{1}{3}})$ will surround x_s, and the interface will not exhibit a sharp discontinuity but will undergo instead a smooth but rapid change in position over a length comparable to the spacing of the plates. The behaviour above and below this singular region should be well represented by the above analysis, however, and the solution of (3.7) should provide a reasonable prediction of the mean position of the 'discontinuity' in the interface.

A physical explanation of the unusual behaviour described mathematically by this analysis can be obtained by viewing the kinematic condition (2.7) as a mass balance over an infinitesimally thin slice of the clear-fluid layer. As mentioned earlier, (2.7) shows that to leading order a dimensionless flux of fluid with magnitude $\sin\theta$ always crosses the interface into the clear-fluid layer and that this new fluid causes an increase in the thickness of the clear-fluid layer (i.e. accumulation), an increase in the flow rate

of pure fluid along this layer, or a combination of these two effects. Furthermore, since the clear-fluid layer is very thin relative to its length, the flow rate through it depends, to leading order, only on its instantaneous local thickness; in fact, the solution of the appropriate momentum equations shows that for a batch process the flow rate is given by

$$\frac{\tilde{b}^3}{3}\tilde{\delta}^3(1-\tilde{\delta})^3\cos\theta. \tag{3.8}$$

Suppose that initially the vessel is completely filled with suspension. Since the transverse component of the bulk velocity vanishes at any x where $\partial\tilde{\delta}/\partial x = 0$ (cf. (2.4*c*) and (2.5)), the particles begin to settle away from the wall with dimensionless velocity $\sin\theta$, the y component of their settling velocity. Hence, initially the flux of fluid across the interface is not due to any bulk motion normal to the interface, but instead results from the motion of the interface due to the particles settling relative to the bulk (it should be remembered that the particle velocity is given by $\mathbf{u}+\mathbf{e}$, where $\mathbf{e}$ is a unit vector in the direction of gravity). Therefore, the thickness of the clear-fluid layer increases linearly with time everywhere except near $x = 0$, where, as already explained in I, $\tilde{\delta}$ must vanish to leading order throughout the process. Thus, near $x = 0$ the interface becomes curved and in this region a transverse bulk flow develops which is strong enough to counterbalance the y component of the particle settling velocity. As a result the interface becomes steady near $x = 0$. We see then that below some point, $x^*(\tau)$, the interface will be at its steady position while above x^* it will be flat and moving with velocity $\sin\theta$ across the vessel. All of the fluid flowing across the interface below $x^*(\tau)$ flows up the clear-fluid layer and is accumulated at the top of the vessel, whereas, above x^*, the production of particle-free fluid is due to the growth of the layer in this region. Note that, at any instant, the constant thickness of the layer above $x^*(\tau)$ is just sufficient to allow all of the particle-free fluid formed below $x^*(\tau)$ to flow through this section of the layer and reach the top. Of course, the accumulation of pure fluid above the suspension leads to an enhanced velocity of the interface at the top of the suspension.

The clear-fluid layer can continue to develop in this manner until $\tau = \frac{1}{2}$, at which time its thickness is half the width of the vessel for all points above $x^*(\frac{1}{2})$. However, as can be seen from (3.8), the flow rate through the clear-fluid layer is at a maximum when $\tilde{\delta} = \frac{1}{2}$. Thus, the region over which the interface is steady cannot lengthen any further since if it did so the fluid crossing the interface over this new steady segment would also have to flow up the layer, thereby increasing the flow rate past its maximum possible value; clearly this is impossible. So the interface must remain flat above $x^*(\frac{1}{2})$ and continue to sweep across the vessel with velocity $\sin\theta$. But, as $\tilde{\delta}$ increases above $\frac{1}{2}$, the flow rate through the clear-fluid layer decreases and all of the new particle-free fluid formed below $x^*(\frac{1}{2})$ can no longer flow through the layer above $x^*(\frac{1}{2})$; i.e. 'extra' pure fluid must accumulate at $x^*(\frac{1}{2})$. This 'extra' fluid then causes the point of discontinuity in the interface, $x^*(\tau)$, to move down the vessel as predicted by (3.7), thereby further increasing the volume of the clear-fluid layer.

All that remains now is to determine the motion of the interface at the top of the suspension. Although the rate at which particle-free fluid is formed is still that given by the PNK theory, the motion of the top of the suspension will be significantly different from that predicted by (1.3) because the thickness of the clear-fluid layer

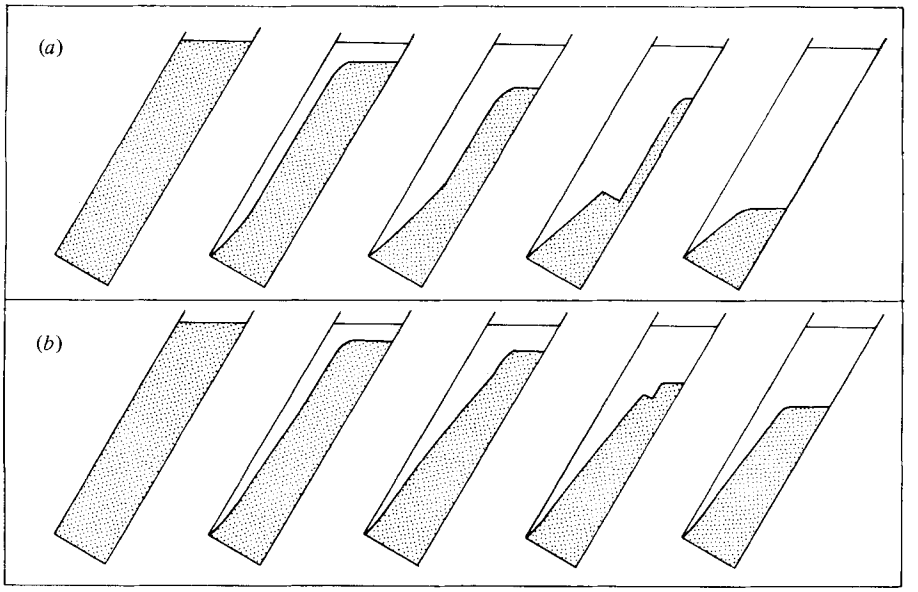

FIGURE 3. Two possible time sequences for the interface position in high-aspect-ratio vessels (time increases left to right). (*a*) The interface along the clear-fluid layer above the point of discontinuity sweeps all of the way across the vessel before the top of the suspension reaches the point of discontinuity. (*b*) The top of the suspension reaches the point of discontinuity before the upper portion of the suspension disappears (i.e. before $\tau = 1$).

becomes an appreciable fraction of the channel width and, throughout most of the process, a large portion of the clear fluid formed accumulates in this layer instead of in the region above the suspension. An expression governing the motion of this part of the interface can be found by applying the jump condition (3.6) with $\tilde{\delta} = 1$ above the jump and $\tilde{\delta} = \tau$ below. Then, noting that $H = x\cos\theta$, we obtain

$$-\frac{dH}{dt} = \Lambda^{\frac{1}{3}}\frac{\tilde{b}^2}{3}\tau^3(1-\tau)^2\cos^2\theta. \tag{3.9}$$

Comparison of (3.9) with the dimensionless form of (1.3), the corresponding PNK result, shows that, due to the accumulation of fluid in the clear-fluid layer, the PNK theory substantially overestimates the velocity of the top of the suspension during the initial stages of the sedimentation process.

Equation (3.9) applies between $\tau = 0$ and either $\tau = 1$ (at which time the region of suspension above x_s has swept clear across the vessel) or the value of τ at which the top of the suspension has descended to the uppermost point of the steady part of the fluid–suspension interface, if this latter condition occurs for $\tau < 1$. These two distinct possibilities are sketched in figure 3. After this time, no further accumulation occurs in the clear-fluid layer, but the PNK theory is still inadequate for predicting the motion of the top of the suspension because the thickness of the clear-fluid layer will, in general, be an appreciable fraction of the width of the channel. In fact, the same type of arguments used above show that $H(t)$ is governed by

$$-\frac{dH}{dt} = \frac{1}{1-\tilde{\delta}_m}\left(1+\Lambda^{\frac{1}{3}}\frac{H}{\tilde{b}}\sin\theta\right)+O(\Lambda^{-\frac{1}{3}}), \tag{3.10}$$

where $$\tilde{\delta}_m = \frac{1}{2}\left(1 - \left(1 - \frac{4}{\tilde{b}}\left[3H\frac{\tan\theta}{\cos\theta}\right]^{\frac{1}{3}}\right)^{\frac{1}{2}}\right).$$

Hence, during this stage of the settling process, the velocity of the top of the suspension is greater than predicted by the PNK theory.

During the course of the experiments described in § 5, it was observed that, in general, the interface does not form a sharp corner at the top of the suspension but instead is somewhat rounded. The present analysis indicates, however, that this broadening of the clear-fluid layer is confined to a region whose dimensions are comparable to the spacing of the plates and, hence, that it has an $O(\Lambda^{-\frac{1}{3}})$ effect on the motion of the top interface. Therefore, (3.9) and (3.10) still apply to leading order.

4. Continuous settling

As discussed in I, the inclined settling process can be used on a continuous basis by adding new suspension with concentration c_0 into the channel while simultaneously removing pure fluid and concentrated sediment. In view of the results of the previous section, however, the feasibility of using high-aspect-ratio vessels for continuous systems might be open to question because it is far from obvious that steady solutions for the flow will exist under all sets of conditions. Fortunately, as we shall see below, it is possible to introduce the new suspension and to remove pure fluid in such a way as to suppress the transient behaviour described in the previous section and to attain, in principle, steady interface shapes for all values of the aspect ratio.

We begin by noting that, in view of (2.7) and (2.8), the conditions governing a steady interface position for continuous settling vessels are given by

$$[1-(3-2\tilde{\delta})\,\tilde{\delta}^2]\left\{Q_f+\int_0^x V(\zeta)\,d\zeta\right\}+(3-2\tilde{\delta})\,\tilde{\delta}^2\left\{Q_s+\int_0^x F(\zeta)\,d\zeta\right\} + \frac{\tilde{b}^3}{3}\tilde{\delta}^3(1-\tilde{\delta})^3\cos\theta = x\sin\theta, \quad (4.1)$$

where $Q(x)$ has been evaluated by integrating (2.6), while Q_f and Q_s denote the dimensionless flow rates at which, respectively, pure fluid is removed from the bottom of the vessel and suspension of volume fraction c_0 is added through the bottom of the vessel. We next introduce the rather obvious restriction that new suspension may only be added to the channel while pure fluid may only be removed from the channel. Therefore each of the two functions

$$Q_f+\int_0^x V(\zeta)\,d\zeta \quad \text{and} \quad Q_s+\int_0^x F(\zeta)\,d\zeta$$

is a monotonically increasing non-negative function of x, and has a maximum value equal to the overall dimensionless volumetric settling capacity of the channel, which from the PNK theory and the analysis of I is equal to $\tan\theta+O(\Lambda^{-\frac{1}{3}})$. Moreover, since $0 \leqslant x\sin\theta \leqslant 1$ and $0 \leqslant (3-2\tilde{\delta})\,\tilde{\delta}^2 \leqslant 1$, it is possible to construct the details of the feed and withdrawal distributions so that a function $\tilde{\delta}(x)$ can clearly be found such that (4.1) is satisfied for all $0 \leqslant x \leqslant \sec\theta$ regardless of the values of $\tilde{b}$ and θ. For example, the case where all the feed is introduced below x_c, cf. (3.3), and all the pure fluid is withdrawn through the top of the channel is one such possibility leading to steady

solutions. Here, as seen from (2.8), the resulting increase in the flow through the clear-fluid layer is sufficient to accommodate all of the fluid produced below any point x. Another possible steady flow regime occurs where the feed is introduced at the top of the vessel and the pure fluid is removed below x_c. Actually, if all or some of the fluid is removed through the bottom of the vessel at $x = 0$, i.e. if $Q_f > 0$, then we see from (4.1) evaluated at $x = 0$ that $\tilde{\delta}(0) = 1$. In other words, the thickness of the suspension layer vanishes at $x = 0$ and the clear-fluid layer extends clear across the vessel.

On the other hand, if all the feed and withdrawals are located at the top of the vessel, then for all $0 \leqslant x < \sec\theta$ the first two terms on the left-hand side of (4.1) vanish and steady solutions exist only if $\sec\theta > x_c$ (i.e. only if $\tilde{b} < (192\tan\theta\sec\theta)^{\frac{1}{3}}$). Whether or not other feed and withdrawal distributions will result in steady interface shapes can be determined, of course, by solving (4.1).

Let us consider briefly the special case when $\tilde{b}$ is greater than $(192\tan\theta\sec\theta)^{\frac{1}{3}}$ and when all of the suspension feed and the pure-fluid withdrawals are located at the top end of the suspension, i.e. at $x = \sec\theta$. Then, $\tilde{\delta}(x)$ is given by (3.2) and, interestingly, two steady solutions are possible: In the first solution, the thickness of the *clear-fluid* layer vanishes at the bottom of the vessel and then grows with x, as is always observed in batch settling experiments, whereas, in the second solution, the thickness of the *suspension* layer vanishes at the bottom of the vessel and then grows with x. This existence of two steady solutions was first reported by Probstein, Yung & Hicks (1977) who developed a model similar to that given here but treated only the case $Q(x) = 0$. These authors argued that the second mode of operation may be advantageous in suppressing the effects of any remixing of the particle-free fluid and suspension which might occur if the interface between these regions became unstable. Indeed, this improved settler efficiency was observed by Probstein & Hicks (1978) who experimentally established the second flow regime in $O(1)$ aspect-ratio channels.† Of course, the conditions in the singular regions at the ends of the suspension region and the relative stability of the two flow patterns will determine which regime is actually observed for a given settler configuration. For example, one condition which must be satisfied if the second mode of operation is to persist is that the thickness of the suspension layer must vanish before the bottom of the channel is reached. If this restriction is not met, the suspension will quickly fill the vessel and the flow pattern will evolve into that of the first regime. Since it is almost impossible to establish initial conditions in a batch process so that the requirement described above is satisfied throughout the duration of the settling process, it is not surprising that the second flow regime is observed in continuous systems only.

5. Experimental observations

Since, to our knowledge, all previous investigations have been restricted to channels with relatively small or moderate aspect ratios so that the discontinuous behaviour of the interface predicted theoretically by the analysis of § 3 has never been observed

† In $O(1)$ aspect-ratio channels, this flow corresponds to a thin suspension layer flowing rapidly down the upward-facing surface with the dimensions of the pure-fluid region being $O(1)$. This flow can then be described mathematically by means of an analysis similar to that in I; the details are given in Herbolzheimer (1980).

experimentally, a series of experiments was conducted in a vessel with parallel flat walls and high aspect ratio so that this prediction could be tested. The channel was 125 cm long, 4 cm wide, and b, the spacing between the plates, was 1 cm. The suspension was composed of close-sized spherical glass beads with mean diameter 137 μm and density 2·42 g ml^{-1} while the suspending fluid was a Newtonian oil mixture with density 0·992 g ml^{-1} and viscosity 0·677 P at 21·6 °C, the nominal temperature of the experiments. The latter were conducted by adding the desired amount of beads and fluid to the vessel, mixing the suspension for several minutes with a plunger-type stirring rod to render the initial concentration distribution nearly uniform, removing the stirring rod, and then quickly tilting the vessel from the vertical to the desired angle of inclination. This procedure was adopted in order to closely approximate the initial conditions used in the theory: namely, that the channel was completely filled with suspension at $t = 0$ (i.e. $\tilde{\delta}(x, 0) = 0$). Detailed observations of the flow field were made for the following range of the parameters:

$$H_0 \approx 90 \text{ cm}, \quad 5° \leqslant \theta \leqslant 45°, \quad 0{\cdot}01 \leqslant c_0 \leqslant 0{\cdot}025,$$

so that $1{\cdot}7 \times 10^7 < \Lambda_0 < 3{\cdot}5 \times 10^7$, $1{\cdot}8 < R_0 < 2{\cdot}1$, and $2{\cdot}4 < \tilde{b} < 3{\cdot}5$. The particle concentrations were kept small because, otherwise, a longer vessel would have been needed in order to observe the discontinuity.

The qualitative features of the flow were identical for all of the conditions investigated. Initially, the suspension was quiescent, but, as the particles began to settle away from the wall (i.e. as the clear-fluid layer began to develop), a rapid motion set in within the clear-fluid layer and within the suspension, where the particle motion was essentially parallel to the walls of the channel. When $\delta(x, t)$, the thickness of the clear-fluid layer was less than half the spacing between the plates, the velocity close to the interface was positive, i.e. directed up the channel, but, as the upward-facing surface was approached for a fixed value of x, the velocity vanished and then became large again but negative. On the other hand, for any value of x where $\delta(x, t) \approx \frac{1}{2}b$, the longitudinal velocity vanished at the interface and was negative within the suspension region. Finally, if $\delta(x, t)$ exceeded $\frac{1}{2}b$, the longitudinal velocity at the interface was also negative. These results are in agreement with the velocity profile predicted in § 2. We should also mention that the sediment layer flowed rapidly down the upward-facing surface of the channel and that its thickness remained small compared to the spacing between the plates throughout the settling process.

Of course, the most startling prediction of our theoretical analysis for batch processes concerns the evolution with time of the thickness of the clear-fluid layer. By using a cathetometer to measure $\delta(x, t)$ as a function of time for several positions along the channel, it was indeed confirmed that in the upper portion of the vessel δ was independent of x but increased with time. Although this measurement of the interface position was subject to considerable experimental error, it appeared that the upper portion of the interface swept across the channel with a velocity which was at least close to $v_0 \sin\theta$, the y component of the particle-settling velocity. The same behaviour occurred in the lower portion of the vessel for small t, but here the interface attained a steady shape after a period of about 0–120 s depending on the value of x and the conditions of the experiment. Over this steady portion of the interface, $\delta(x)$ increased monotonically with x and was vanishingly small at $x = 0$ throughout the process. When δ became equal to about half the spacing between the plates, the predicted

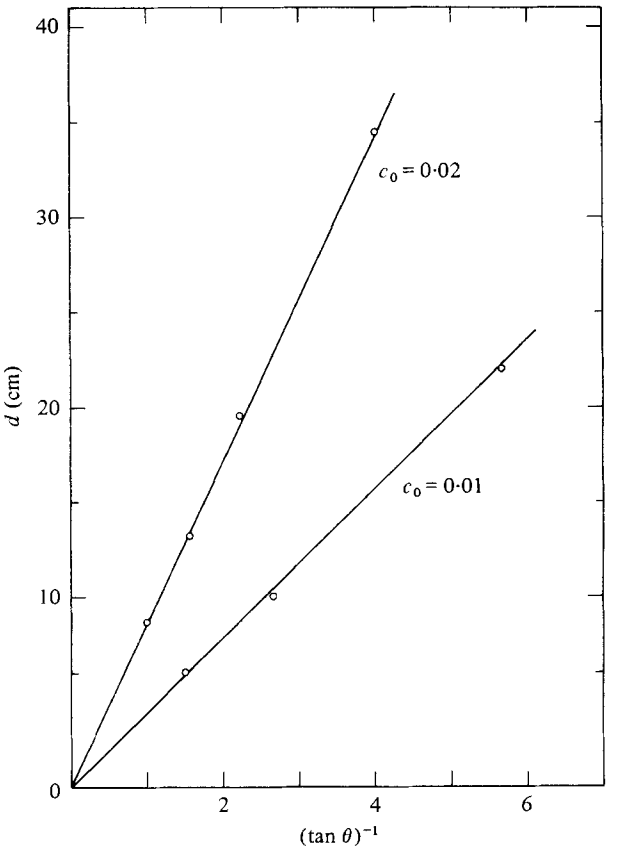

FIGURE 4. The distance, measured along the downward-facing surface of the vessel, from the bottom of the vessel to the point of discontinuity in the thickness of the clear-fluid layer, at the instant when the upper portion of the suspension region first disappears, versus $1/\tan\theta$: $b = 1$ cm; $c_0 = 0{\cdot}01$ and $0{\cdot}02$. The solid lines are the corresponding theoretical predictions obtained from (5.1).

'discontinuity' in δ as a function of x begin to develop, with δ remaining time-independent below this point of 'discontinuity'; in contrast, beyond this point, δ was independent of x but continued to increase with time. Once the 'discontinuity' appeared, its position continually moved down the channel with time. Of course, as would be expected, the thickness of the clear-fluid layer did not undergo a sharp jump in the region of the discontinuity, but instead grew rapidly over a distance comparable to the spacing between the plates. This is consistent with the fact that the point of discontinuity is surrounded by a singular region with dimensions $O(\Lambda^{-\frac{1}{3}})$ in which the length scales in both the x and y directions are comparable.

In a typical case, then, approximately the top three-quarters of the suspension disappeared (i.e. became settled) after about 2–3 minutes and only a small quasi-steady region, which subsequently settled in a manner similar to that in $O(1)$ aspect-ratio channels, remained in the bottom fourth of the vessel. Note that, if the vessel had been left vertical, more than an hour would have been required to settle this same amount of suspension. We should emphasize that the top region of the suspension disappeared

because the particles settled into the wall and not because the top of the suspension travelled down the channel. This top interface did fall with an enhanced velocity, but as was predicted by (3.9), this velocity was considerably lower than that which would have been expected on the basis of the PNK theory.

The results so far are all in excellent agreement with the predictions of § 3. The only real question remaining is whether or not the theory can quantitatively predict the location of the point of discontinuity. Unfortunately, the exact location of the discontinuity cannot be discerned for a while after it has developed because, initially, the jump in the thickness of the clear-fluid layer at this point is too small to be observable. Hence, it was decided to measure instead the location of the point of discontinuity at the instant when the portion of the interface above this point first reached the upward-facing wall of the channel. This is actually a more stringent test of the theory because it also tests the validity of (3.7), the equation governing the motion of the discontinuity. Therefore, if we let d denote the distance (measured along the vessel) from the bottom of the channel to the top of the suspension at this instant, we obtain from the numerical solution of (3.7) that d should satisfy

$$d = 0{\cdot}571 \times \frac{3}{128} \frac{b^3}{a^2} \frac{1}{\tan\theta} \frac{c_0}{f(c_0)}. \tag{5.1}$$

Experimentally measured values of d are plotted in figure 4 as a function of $(\tan\theta)^{-1}$ for values of c_0 equal to 0·01 and 0·02. The solid lines are the theoretical predictions obtained from (5.1) by using the correlation of Barnea & Mizrahi (1973) to evaluate $f(c_0)$. Clearly, the agreement is excellent, indicating that, at least for dilute suspensions, the theory presented in §§ 2 and 3 provides a quantitative as well as qualitative understanding of sedimentation in narrow inclined channels.

This work was supported in part by contract EPRI-RP-314-1 with the Electric Power Research Institute in Palo Alto, California, and by the National Science Foundation under Grant ENG 78-16928.

REFERENCES

Acrivos, A. & Herbolzheimer, E. 1979 Sedimentation in settling tanks with inclined walls. *J. Fluid Mech.* **92**, 435–457.

Barnea, E. & Mizrahi, J. 1973 A generalized approach to the fluid dynamics of particulate systems: Part 1. General correlation for fluidization and sedimentation in solid multiparticle systems. *Chem. Engng J.* **5**, 171–189.

Boycott, A. E. 1920 Sedimentation of blood corpuscles. *Nature* **104**, 532.

Herbolzheimer, E. 1980 Enhanced sedimentation in settling vessels having inclined walls. Ph.D. dissertation, Stanford University.

Nakamura, N. & Kuroda, K. 1937 La cause de l'accélération de la vitesse de sédimentation des suspensions dans les récipients inclinés. *Keijo J. Med.* **8**, 256–296.

Ponder, E. 1925 On sedimentation and rouleaux formation. *Quart. J. Exp. Physiol.* **15**, 235–252.

Probstein, R. F. & Hicks, R. E. 1978 Lamella settlers: a new operating mode for high performance. *Ind. Water Engng* **15**, 6–8.

Probstein, R. F., Yung, D. & Hicks, R. E. 1977 A model for lamella settlers. Presented at 'Theory, Practice, and Process Principles for Physical Separations', Engng Foundation Conf., Asilomar, California.